A simple solution to imaging of bioprinted constructs

Sönke Menke[1,2,*], Hanne Hjorth Tønnesen[1], Tomasz Jüngst[2] and Krister Gjestvang Grønlien[1]

[1] Section for Pharmaceutics and Social Pharmacy, Department of Pharmacy, University of Oslo, P.O. Box 1068 Blindern, NO-0316 Oslo, Norway, [2]Department for Functional Materials in Medicine and Dentistry at the Institute of Functional Materials and Biofabrication (IFB) and Bavarian Polymer Institute, University of Würzburg, 97070 Würzburg, Germany

*corresponding author

E-mail: soenke.menke@epfl.ch

A simple solution to imaging of bioprinted constructs

Efficient development of printable inks for extrusion-based 3D bioprinting is a major issue in biofabrication. Commonly used inks are often comprised of polymer solutions that form hydrogels under the addition of water and additives such as crosslinkers. Once an extrudable ink is identified, the printing parameters must be optimized for each inks' specific composition. An important method for the assessment of printability is imaging of printed samples. Here we introduce and discuss an easy-to-use printable device for the imaging of bioprinted samples. The use of the device was demonstrated by printing and imaging inks with different compositions. The obtained images were compared to those of a stereomicroscope traditionally used for the imaging and evaluation of bioprinted constructs. When compared, it was found that the new imaging device produced results that were of comparative, if not better quality than the stereomicroscope, while costing less than $50 (mobile device for imaging not included), as well as showing increased convenience due to its smaller size, portability, and customisation capabilities. We propose that this new device can be used for benchtop evaluation of bioprinted constructs as well as in the scope of teaching of biofabrication classes.

Keywords: bioprinting; imaging; 3D printing; Pluronic F-127; open-source

1. Introduction

Throughout the recent years, 3D printing; also known as additive manufacturing (AM), has greatly increased in popularity and become a well-known term throughout the general population. While the global market size was valued at $4.4 billion in 2013, this number rose to more than $14 billion in 2020 with an expected compound annual growth rate of 21 % from 2021 to 2028.[1,2] The field of AM is very diverse and many different technologies fall under the umbrella of 3D printing. Due to this, the terms are often confused amongst the broad audience.[3] The most common techniques used in AM are fused deposition modelling (FDM), digital light processing (DLP), and selective laser sintering (SLS).[2,4] The latter is already used in the medical field for the production of titanium hip implants.[5,6] Thus, AM is regarded as the next manufacturing revolution.[7]

One emerging field in the area of AM is biofabrication, which has gained significant attention in the recent years. It was defined as "*the automated generation of biologically functional products with structural organization from living cells, bioactive molecules, biomaterials, cell aggregates such as micro-tissues, or hybrid cell-material constructs, through Bioprinting or Bioassembly and subsequent tissue maturation processes*" in 2016 by Groll *et al*.[8] In order to print such constructs, suitable bio (material) inks must be developed. It is important to differentiate between inks with and without the content of living material. An aqueous formulation of hydrogels or polymers used in bioprinting is called a biomaterial ink, whilst the addition of cells into the ink leads to what is known as a bioink.[9] In bioprinting, hydrogels are often the preferred base material. Hydrogels are three-dimensional networks of polymers able to hold large amounts of water.[10] They can absorb from as little as 30 % up to a thousand times their dry weight of water.[11,12] This creates an environment reminiscent of natural tissues, allowing the cells to adhere, proliferate and differentiate.

There are two common categories of base materials being used: synthetic polymers, such as polycaprolactone, polyoxazolines/polyoxazines, poloxamers and polyethylene glycol, and biomacromolecules from natural sources like plants, bacteria, cells and animals, such as collagen, alginate and pectin.[9,13,14] The inks should have shear thinning properties, while not being thixotropic, and should not exhibit swelling properties post extrution.[3,15] Furthermore, a bioink must have a low enough viscosity before printing to allow for mixing and homogeneous distribution of cells before and throughout the printing process. Additionally, the viscosity must be low enough that the resulting shear forces do not affect the viability of the cells.[3] Once a promising ink formulation has been found, the printability needs to be tested and the shape fidelity analysed, as the printed construct should be able to exhibit the desired shape and retain

it.[16] One product that is often used as a comparative baseline for the newly developed inks is Nivea® crème, as it is mass manufactured and exhibits superior properties for printing.[16] During the printing process, the final outcome is greatly influenced by the following parameters: print speed, head temperature, bed temperature, nozzle/needle diameter, extrusion rate (often expressed as pressure), and height of the first layer. When printing a new material, these parameters must be assessed individually.[16] As an example, Diamantides *et al*. (2017) used a system of printing a line, a square and multiple stacked squares (cuboid) to evaluate printability of a collagen-based bioink.[17] After completing such test prints, they must be imaged and analysed. Imaging is often carried out using stereomicroscopes, which are especially useful when imaging small objects. Since most bioprinted constructs during test prints are in the millimetre-range, there are a large variety of imaging techniques available. The most traditional approach however, is through the use of an optical microscope. In recent years, due to the rapid increase in smartphone technologies utilising high-end processors and cameras, more and more researchers have started using mobile devices in place of spectrometers and microscopes.[18–23] This can be especially advantageous in the field of education as modern instruments are often expensive while constructs on the macro scale might not require the resolution of modern microscopes.

In the present work, we aimed to develop an open-source affordable, simple imaging device for evaluation of bioprinted constructs. The device consisted of a simple, portable, and low-cost box, which may be used in conjunction with the imaging capabilities of modern mobile devices. The device was developed to create 16 different lighting environments, allowing the phone to image printed samples with an accuracy comparable to that of a microscope. As proof of concept, samples of 6 different materials, based on Pluronic® F-127, and a Nivea® crème as a control were printed and

subsequently imaged. Due to the ease in construction, this allows for usage in education while teaching fundamental knowledge in 3D printing, electronics, and bioprinting.

2. Materials and Methods

2.1 FDM printing

To create individual parts, a Zmorph VX (Zmorph S.A., Wrocław, Poland) FDM printer with Poly(lactic acid) (PLA) filament was used. The models were designed in Fusion360 (Autodesk Inc., Dublin, Ireland) and sliced with Voxelizer3 (Zmorph S.A., Wrocław, Poland). The printing parameters were adopted form the software, only infill, density and quality were changed according to the needs.

2.2 Biomaterial printing

A Bio X™ (Cellink AB, Gothenburg, Sweden) bioprinter was used with a thermally controlled printhead to print biomaterials inks. As surface for bioprinting, Menzel-Gläser 35 x 76 x 1 mm glass slides (Menzel GmbH & Co KG, Braunschweig, Germany) were used. The print parameters were changed according to the material to achieve optimal print quality. A 20 G blunt needle was used (inner diameter (ID): 0.58 mm). The glass slides were held with a custom-made frame to accommodate three glass slides at a time (3D files available in the Supporting Information, SI). The G-code used to print three test structures on three slides in one run can be found in the SI.

2.3 Ink formulation

Nivea® hand cream (Beiersdorf AG, Hamburg, Germany) was used as received. Poloxamer 407 was purchased as Pluronic® F-127 from BASF (BASF SE, Ludwigshafen am Rhein, Germany). Rose bengal and methylene blue (Sigma-Aldrich Chemical

Company, St. Louis, MO, USA) were purchased from Merck KGaA (Darmstadt, Germany). To create the biomaterial inks, a 22 or 35 % (w/v) solution in water (Milli-Q) was refrigerated for 24 h at 5 °C prior to transferral into 3 mL cartridges (Cellink AB, Gothenburg, Sweden). Samples containing dyes were prepared with either rose bengal, or methylene blue (0.1 g/L respectively). The dye was added prior to refrigeration. In preparation for printing, all samples were placed inside a degassing station (7 °C, 5 min, 635 mm Hg, Waters Coop., TA Instruments, New Castle, USA) to remove air bubbles.

2.4 Imaging

For Imaging, a Leica MZ16 Microscope (Leica Microsystems GmbH, Wetzlar, Germany), a OnePlus 7T Pro (OnePlus Co. Ltd., Shenzhen, PR China), and an iPhone 13 Pro Max (Apple Inc., CA, USA) was used. The phones were used in 'macro' setting.

2.5 Experimental Set-Up

To simplify the imaging of printed constructs, a device was created (see Figure 1. For more information regarding the building process, see SI). In order to light up the glass slides, light-emitting diodes, 5 mm, white (LEDs, Luxorparts, Malmö, Sweden) were installed (detailed building plans can be found in the SI). This array of 12 LEDs in 4 different circuits can be used to create 16 lighting situations (see Table S1 in the SI).

The imaging-device was designed to be compatible with different smartphones by the application of phone-specific inserts. Inserts for the iPhone 13 Pro Max and the OnePlus 7T Pro were prepared, but the design is easily adaptable for other devices. Every phone must be calibrated in order to create accurate scales to support the images (see SI).

2.6 Image analysis

Evaluation of the printed constructs was carried out by taking pictures using a smartphone with the imaging device, subsequent analysis of the images was then conducted using Fiji ImageJ.[24] This process was automated as far as possible using macro commands. During this process, a threshold was set manually, as this is a variable that cannot be fully automated at this stage. This threshold defines the grey value pixels should have to be counted as particles and helps select the structures that are to be analysed. A set of macros were written, which processed the pictures up to this point. The final version of the macros can be found in the SI. While the area is a value that ImageJ can determine independently, the width of the line must be determined with alternate methods. In this case, the average width was determined using the plugin local thickness.[25]

2.7 Statistical analysis

The data is presented as mean ± standard deviation (SD). Experiments were performed once with three technical replicates. Statistical analyses were performed by using Student's t-test in GraphPad Prism version 9.1.0 for Windows (GraphPad Software, La Jolla, CA, USA; www.graphpad.com). Differences were considered significant at $p < 0.05$.

3. Results

Evaluating bio(material) ink printability reveals that each measured parameter has significant effects on the quality of the printing output. Therefore, all variables must be individually analysed. For this purpose, specific G-codes were written to gradually alter the parameters: speed, pressure, and height of the first layer (see SI). An example of this optimisation process, printed with Nivea cream, can be found in Figure 2a. After suitable

parameters were found, The shape fidelity for the respective biomaterial inks was assessed using methods similar to that of Diamantides *et al*. (2017).[17] Three shapes were printed: a 5 mm line, a 5 x 5 mm square and three of those squares, stacked on top of each other (further referred as a cuboid). The code for these shapes can be found in the SI. For cuboid and square, the area is the relevant parameter which will be compared, as it shows the precision of the print, while for the line, the average width is important. The samples were imaged using the imaging device. Throughout our testing procedures, it was determined that three of the lighting situations provided the most illuminating data (see Figure 2b-d).

Samples were printed using colourless, red, and blue Pluronic® inks, as well as Nivea cream as comparison. For square and cuboid, the mean area (n = 3) was compared to the theoretical area, while the mean line width (n = 3) was compared to the needle diameter (see Figure 3).

4. Discussion

The imaging device was designed to be easy to use and manufacture. If needed, parts can be replaced or altered to fit better with alternative requirements. The printing of the device was possible to complete in less than 2 days. The lighting situation can also be altered by the installation of more LEDs and by using coloured LEDs. By the application of LEDs with specific wavelengths, the device could also be used for crosslinking and/or fluorescence imaging after minimal alterations as previously reported by Anand and co-workers (2022).[23] Further automatization is possible by using a Raspberry Pi with a camera that can transmit the images wirelessly to a computer, a technology that is already gaining traction in a variety of applications.[26] Another possibility would be to analyse the images directly through an app.

By using different imaging backgrounds, the contrast can also be increased. To make this easier, the background was made as a separate file, which can be printed within 15 min in different colours. Since the main power source is a 9V block battery, the device can be used without connection to mains electricity, which makes it versatile and possible to be used everywhere. Together with the small footprint, the application of the device in fume hoods or sterile workbenches should be possible without further issues. Since the device material can easily be altered, alternatives that are autoclavable or that can be sterilized using other techniques may be selected. By storing the battery in one of the side panels instead of outside the device, the possibilities for such use increases. The limiting factor of the device is the phone and its camera. By using a phone with a better camera, the resolution increases, as well as the dynamic range, which makes the analysis easier. Another drawback with the arrangement of the top lights, is the creation of a shadow on the glass slide. This could lead to issues with some samples that are as big as the whole glass slide. More LEDs can easily be added to combat this problem.

Minor technical development is required within the analysis stage of the experiment. The software occasionally faced challenges in detecting the correct pixels due to noise or low contrast. In such instances, manual adjustments were applied to the images to ensure accurate shape detection. An illustrative case can be found in Figure 2a, where the middle structure, printed with adequate line width, unfortunately remained incompletely closed (visible in the upper left corner). This rendered ImageJ incapable of determining the areal measurement. To address this, a simple solution was employed – the addition of a few white pixels. This correction, while having minimal impact on the procedure's viability, is crucial for maintaining result accuracy. If numerous line corrections are necessary, the experiment must be repeated with new light settings or a different analysis approach. This issue is a problem on the printing side of the process

and less on the analysis and imaging part. Unfortunately, the use of the imaging-device method does not rectify the drawback common to microscopy analysis in which translucent materials in low contrast images pose issues to the ImageJ analysis software.

When comparing the results of the tested samples that were imaged using a microscope and the imaging device, it can be clearly seen that the measurements very often are similar. An unpaired t-test showed that none of the values achieved using the imaging device differ statistically significant from the values from the microscope apart from the Nivea cream cuboid (see Figure 3a, $p < 0.005$). For all Pluronic® inks, the results were similar and therefore, a high precision of both methods can be derived. As the real values for the size of the individual samples are unknown, no statement about the accuracy of the methods can be made. It can be assumed that the methods are sufficient accurate, as all measurements are within a reasonable limit around the theoretical value (on average less than 10 % error, for Pluronic® inks < 2 %). This shows that both the new imaging device and the traditional microscope can be used to image bioprinted samples. In regard to the workflow, it has to be added that the images taken with the phone were easier to analyse, as there were always three objects in one image, while only one structure could be analysed at the time with the microscope due to the lowest zoom setting (see Figure 4).

5. Conclusions

We have successfully demonstrated an easy to manufacture device for the imaging of bioprinted samples. Due to the manufacturing process with FDM, quick and easy adaptation of the design, different applications are possible. When comparing the new imaging device to a conventional microscope, the imaging device has several advantages; it is easy to handle and transport, it is intuitive to operate and presents results comparative

to, if not better than those from a microscope. Furthermore, the results for most samples showed no statistically significant differences between the imaging device and the stereomicroscope. The proposed device can easily be used in the early development steps of bioinks and high throughput screening of new inks. Also an application in an educational setting might show students how to build their own device and use it in classroom during biofabrication classes.

Acknowledgments

The authors would like to thank Ivar Grove, Department of Pharmacy, University of Oslo for technical support and Courtney-Elyce Lewis, Centre for Materials Science, Queensland University of Technology for valuable discussions. S.M. would like to acknowledge the founding provided by ERAMUS+ for his work at Department of Pharmacy, University of Oslo.

References

1. Statista Inc. Global 3D printing market size 2013-2021 | Statista. Available at https://www.statista.com/statistics/796237/worldwide-forecast-growth-3d-printing-market/ (2022).
2. Grand View Research, Inc. 3D Printing Market Size, Share | Industry Report, 2021-2028. Available at https://www.grandviewresearch.com/industry-analysis/3d-printing-industry-analysis (2022).
3. Jungst, T., Smolan, W., Schacht, K., Scheibel, T. & Groll, J. Strategies and Molecular Design Criteria for 3D Printable Hydrogels. *Chem Rev* **116,** 1496–1539; 10.1021/acs.chemrev.5b00303 (2016).
4. Moroni, L. *et al.* Biofabrication: A Guide to Technology and Terminology. *Trends Biotechnol* **36,** 384–402; 10.1016/j.tibtech.2017.10.015 (2018).
5. Kim, D. *et al.* Sacral Reconstruction with a 3D-Printed Implant after Hemisacrectomy in a Patient with Sacral Osteosarcoma: 1-Year Follow-Up Result. *Yonsei Medical Journal* **58,** 453–457; 10.3349/ymj.2017.58.2.453 (2017).
6. Okolie, O., Stachurek, I., Kandasubramanian, B. & Njuguna, J. 3D Printing for Hip Implant Applications: A Review. *Polymers* **12**; 10.3390/polym12112682 (2020).

7. Berman, B. 3-D printing: The new industrial revolution. *Business Horizons* **55,** 155–162; 10.1016/j.bushor.2011.11.003 (2012).

8. Groll, J. *et al.* Biofabrication: reappraising the definition of an evolving field. *Biofabrication* **8,** 13001; 10.1088/1758-5090/8/1/013001 (2016).

9. Groll, J. *et al.* A definition of bioinks and their distinction from biomaterial inks. *Biofabrication* **11,** 13001; 10.1088/1758-5090/aaec52 (2018).

10. Caliari, S. R. & Burdick, J. A. A practical guide to hydrogels for cell culture. *Nat. Methods* **13,** 405–414; 10.1038/nmeth.3839 (2016).

11. Drury, J. L. & Mooney, D. J. Hydrogels for tissue engineering: scaffold design variables and applications. *Biomaterials* **24,** 4337–4351; 10.1016/S0142-9612(03)00340-5 (2003).

12. Park, J. B. & Lakes, R. S. *Biomaterials. An introduction.* 3rd ed. (Springer, New York, 2010).

13. Hahn, L. *et al.* An Inverse Thermogelling Bioink Based on an ABA-Type Poly(2-oxazoline) Amphiphile. *Biomacromolecules* **22,** 3017–3027; 10.1021/acs.biomac.1c00427 (2021).

14. Valot, L., Martinez, J., Mehdi, A. & Subra, G. Chemical insights into bioinks for 3D printing. *Chem. Soc. Rev.* **48,** 4049–4086; 10.1039/c7cs00718c (2019).

15. Dreiss, C. A. Hydrogel design strategies for drug delivery. *Curr. Opin. Colloid Interface Sci.* **48,** 1–17; 10.1016/j.cocis.2020.02.001 (2020).

16. Paxton, N. *et al.* Proposal to assess printability of bioinks for extrusion-based bioprinting and evaluation of rheological properties governing bioprintability. *Biofabrication* **9,** 44107; 10.1088/1758-5090/aa8dd8 (2017).

17. Diamantides, N. *et al.* Correlating rheological properties and printability of collagen bioinks: the effects of riboflavin photocrosslinking and pH. *Biofabrication* **9,** 34102; 10.1088/1758-5090/aa780f (2017).

18. Asheim, J., Kvittingen, E. V., Kvittingen, L. & Verley, R. A Simple, Small-Scale Lego Colorimeter with a Light-Emitting Diode (LED) Used as Detector. *J. Chem. Educ.* **91,** 1037–1039; 10.1021/ed400838n (2014).

19. Kim, H. *et al.* Smartphone-based low light detection for bioluminescence application. *Scientific reports* **7,** 40203; 10.1038/srep40203 (2017).

20. Smith, Z. J. *et al.* Cell-phone-based platform for biomedical device development and education applications. *PloS one* **6,** e17150; 10.1371/journal.pone.0017150 (2011).

21. Switz, N. A., D'Ambrosio, M. V. & Fletcher, D. A. Low-cost mobile phone microscopy with a reversed mobile phone camera lens. *PloS one* **9,** e95330; 10.1371/journal.pone.0095330 (2014).

22. Wei, Q. *et al.* Imaging and sizing of single DNA molecules on a mobile phone. *ACS nano* **8,** 12725–12733; 10.1021/nn505821y (2014).

23. Anand, G., Thyagarajan, T. & Sabitha, R. Fluorescence Nano Particle Detection in a Liquid Sample Using the Smartphone for Biomedical Application. *J Fluoresc* **32,** 135–143; 10.1007/s10895-021-02799-w (2022).

24. Schindelin, J. *et al.* Fiji: an open-source platform for biological-image analysis. *Nat Methods* **9,** 676–682; 10.1038/nmeth.2019 (2012).

25. ImageJ: Local Thickness. Available at https://imagej.net/plugins/local-thickness (2007).

26. Abid, H. A. *et al.* Low-cost Imaging of Fluorescent DNA in Agarose Gel Electrophoresis using Raspberry Pi cameras. *J Fluoresc* **32,** 443–448; 10.1007/s10895-021-02884-0 (2022).

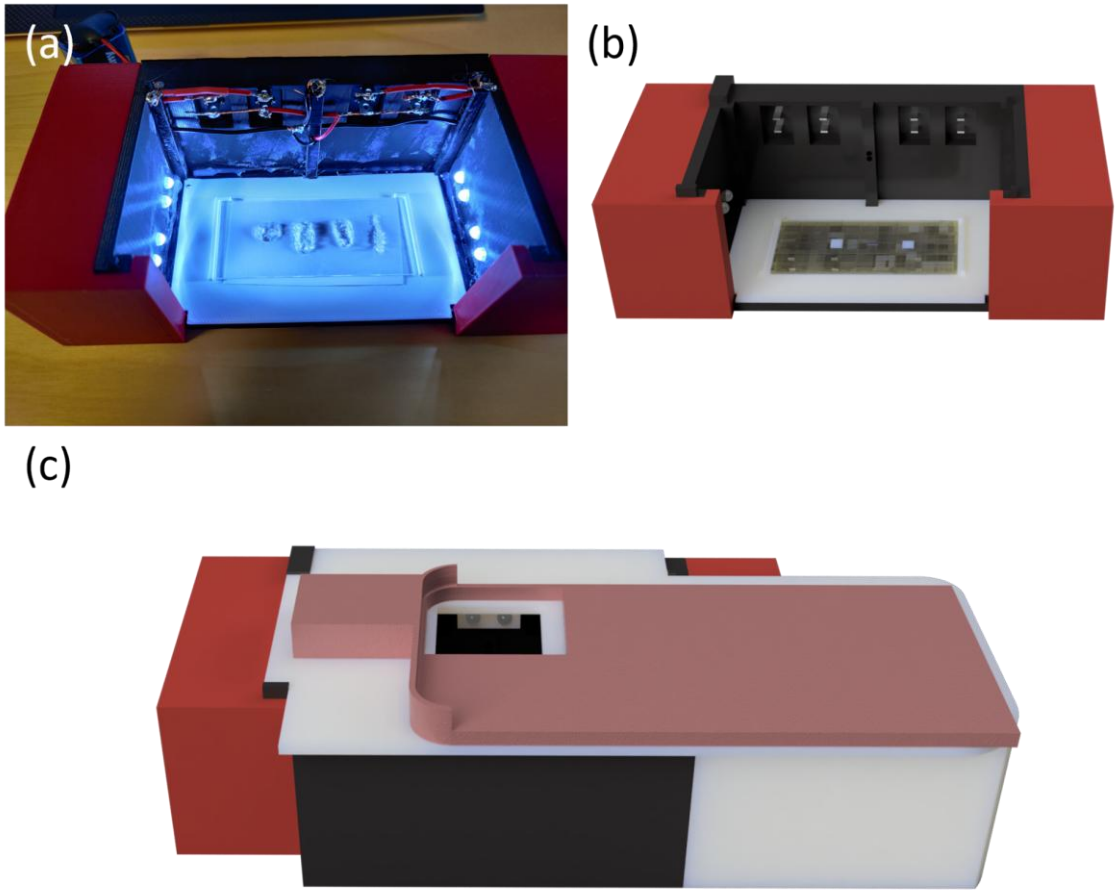

Figure 1. Images of the finished imaging device, equipped with the lid for a OnePlus 7T pro in a) the fully open composition, and render images in the b) fully open and c) fully closed composition.

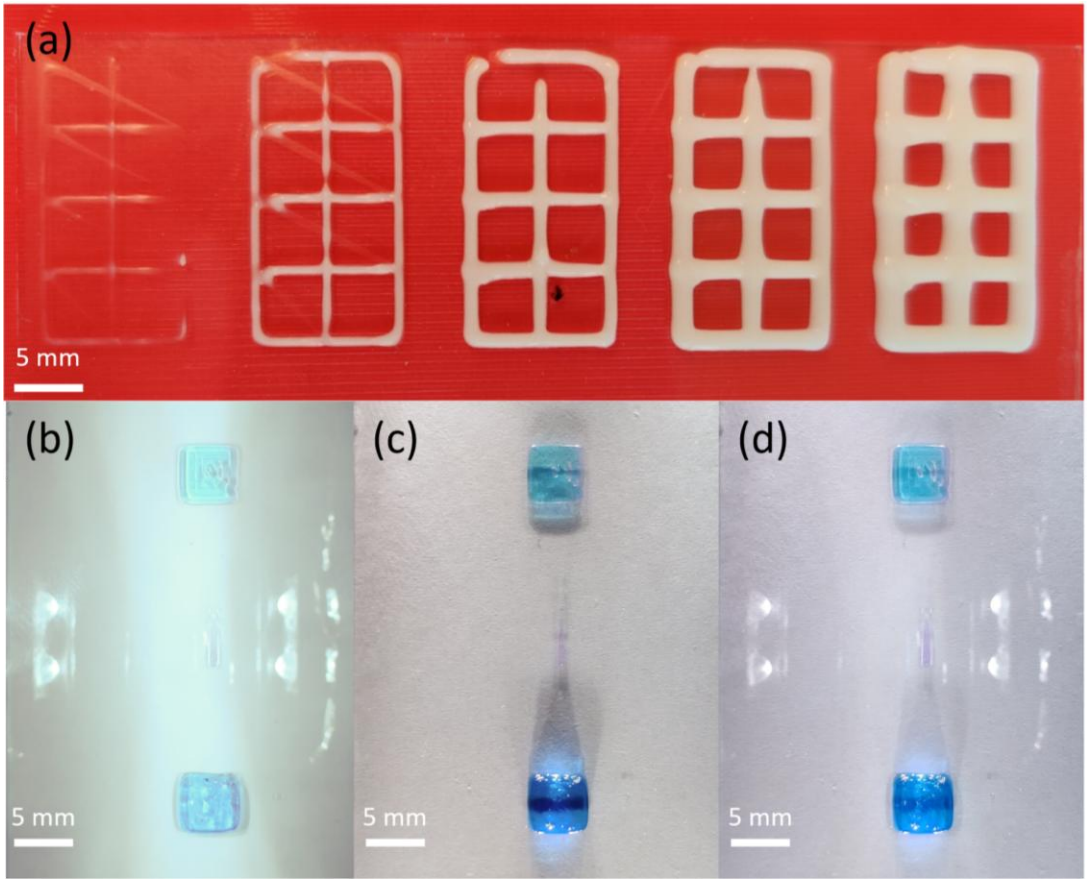

Figure 2. (a): Effects of pressure (20 – 60 kPa right to left in 10 kPa increments) on Nivea crème test prints (speed: 5 mm/s, height of first layer: 2/3 of needle size). (b)-(d): Three different lighting situations, produced with the imaging device and the blue ink containing 35 % (w/v) Pluronic. (b) Top lights on, (c) all lights on, (d) bottom lights on. The white balance was set manually, resulting in different shades of blue.

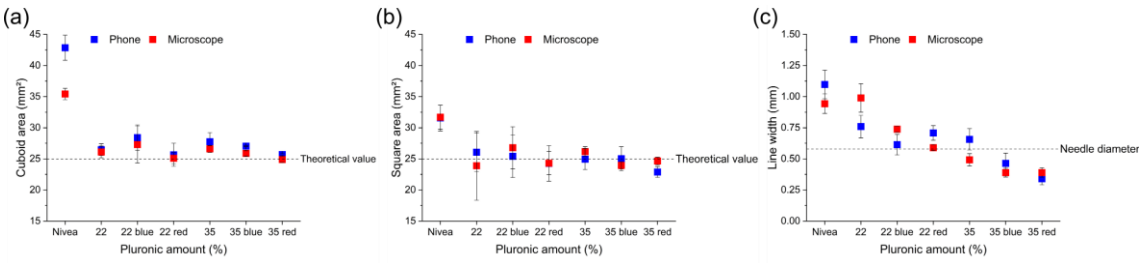

Figure 3. Comparison of the shape fidelity. The samples were imaged using a phone on the imaging device, or a microscope. The area of **(a)** cuboids and **(b)** square are compared to the theoretical value of the model, while the width of the line **(c)** is compared to the needle diameter. Print speed: 5 mm/s, first layer height: 2/3 of the

needle diameter, temperature/pressure: dependant on ink type (see table S2). The values are presented as mean ± SD with n = 3.

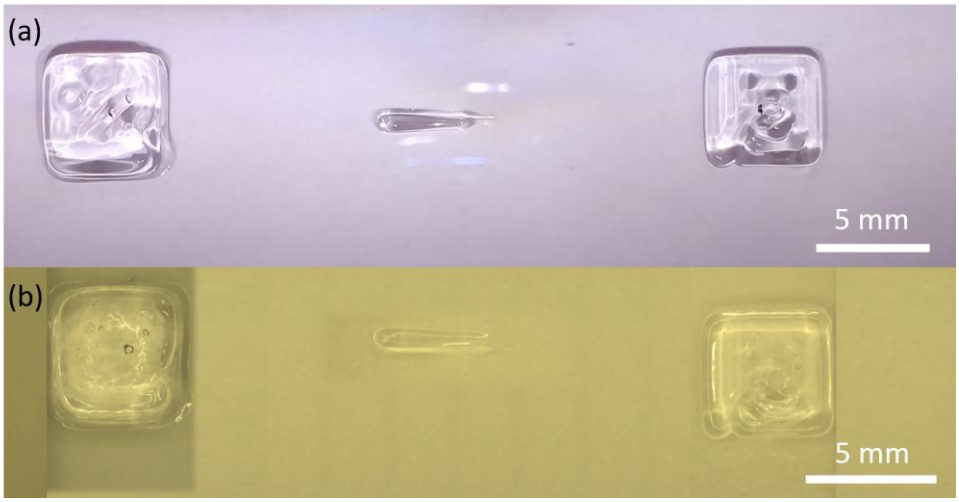

Figure 4. Comparison of the single image taken with the new imaging device (a) and the three images taken with the microscope, stitched together (b).